Analysis of climate change impacts on lake ice phenology in Canada using the historical satellite data record

Article in Remote Sensing of Environment · February 2007

DOI: 10.1016/j.rse.2006.09.015

2 authors:

Rasim Latifovic
Natural Resources Canada
111 PUBLICATIONS 2,855 CITATIONS

D.A. Pouliot
Environment and Climate Change Canada, Ottawa
59 PUBLICATIONS 1,449 CITATIONS


VOLUME 106
ISSUE 4
28 FEBRUARY 2007
ELSEVIER
Remote Sensing of Environment
http://www.elsevier.com/locate/rse

Available online at www.sciencedirect.com
ScienceDirect

Remote Sensing of Environment 106 (2007) 492–507

Remote Sensing of Environment

www.elsevier.com/locate/rse

Analysis of climate change impacts on lake ice phenology in Canada using the historical satellite data record

Rasim Latifovic *, Darren Pouliot

Natural Resources Canada, Canada Centre for Remote Sensing, 588 Booth Street Ottawa, Ontario, Canada K1A 0Y7

Received 1 June 2006; received in revised form 13 September 2006; accepted 16 September 2006

Abstract

Variability and trends in lake ice dynamics (i.e. lake ice phenology) are related to climate conditions. Climate influences the timing of lake ice melt and freeze onset, ice duration, and lake thermal dynamics that feedback to the climate system initiating further change. Phenology records acquired in a consistent manner and over long time periods are required to better understand variability and change in climate conditions and how changes impact lake processes. In this study, we present a new technique for extracting lake ice phenology events from historical satellite records acquired by the series of Advanced Very High Resolution Radiometer (AVHRR) sensors. The technique was used to extend existing in-situ measurements for 36 Canadian lakes and to develop records for 6 lakes in Canada's far north. Comparison of phenology events obtained from the AVHRR record and in-situ measurements show strong agreement (20 lakes, 180 cases) suggesting, with high confidence especially in the case of break-up dates, the use of these data as a complement to ground observations. Trend analysis performed using the combined in-situ and AVHRR record ~ 1950–2004 shows earlier break-up (average — 0.18 days/year) and later freeze-up (average 0.12 days/year) for the majority of lakes analyzed. Less confidence is given to freeze-up date results due to lower sun elevation during this period making extraction more difficult. Trends for the 20 year record in the far north showed earlier break-up (average 0.99 days/year) and later freeze-up (average 0.76 days/year). The established lake ice phenology database from the historical AVHRR image archive for the period from 1985 to 2004 will to a certain degree fill data gaps in the Canadian in-situ observation network. Furthermore, the presented extraction procedure is not sensor specific and will enable continual data update using all available satellite data provided from sensors such as NOAA/AVHRR, MetOp/AVHRR, MODIS, MERIS and SPOT/VGT.

Keywords: Climate change; Remote sensing; Lake ice; Trend analysis

1. Introduction

The most practical climate change indicators are simple measurements that are known to be strongly influenced by climatic conditions. Changes in snow cover, the position of glacier fronts, and lake and river ice duration are examples of useful climate change indicators within the hydrologic system. Variability and trends in lake ice dynamics such as break-up, freeze-up, ice-on, and ice-off durations (i.e. phenology) are clear and direct indicators that can be related to climate condition and lake physical characteristics. It has been shown that lake phenology is a good proxy for past local climate and in some cases can be considered a more robust measure than air temperature (Livingstone, 1997). Furthermore extensive studies of Scott (1964), McFadden (1995), Maslanik and Barry (1987), Robertson (1989), Magnuson et al. (1990), Schindler et al. (1990), and Anderson et al. (1996) report a strong correlation between lake ice phenology and climate variability. The relation is evident at different temporal scales as short-term variability caused by atmospheric conditions, oceanic oscillations and volcanic eruptions as well as long-term variability caused by the general warming trend since the beginning of the last century. Magnuson et al. (2000) analyzed 150-year historical trends in ice cover of 39 lakes and rivers in the northern hemisphere and found that freeze-up dates averaged 0.058 days/year later and change in break-up dates averaged 0.065 days/year earlier using

* Corresponding author.
E-mail address: Rasim.Latifovic@geocan.nrcan.gc.ca (R. Latifovic).

0034-4257/$ - see front matter. Crown Copyright © 2006 Published by Elsevier Inc. All rights reserved.
doi:10.1016/j.rse.2006.09.015

ground observations. Anderson et al. (1996) found that break-up occurred 0.82 days/year earlier for lakes in Southern Wisconsin and 0.45 days/year for lakes in Northern Wisconsin. Schindler et al. (1990) reported a decrease in ice duration for lakes in Northern Ontario at a rate of 1.11 days/year. More recently, Duguay et al. (2006) evaluated trends in break-up and freeze-up for Canadian lakes and found that the majority of lakes in Canada showed earlier break-up and later freeze-up dates. However, results for freeze-up were not as statistically significant and were more spatially heterogeneous. These studies support the general expectation that under climate warming, earlier break-up and later freeze-up are expected, thereby reducing the period of ice-on conditions. This has important implications for local and global climate, energy balances, and chemical, biological, and hydrological cycles. For example, longer ice-off conditions increase the period of direct heat transfer between lakes and the atmosphere, increase the time for which lakes act as a source of greenhouse gases due to chemical and biological processes, and increase the annual evaporation from the lake surface.

Considering the large area that lakes cover both globally and in Canada, a significant influence resulting from lake feedbacks to climate change is possible (Magnuson et al., 1997; Brown & O'Neill, 2002; Rouse et al., 2005). Furthermore, the prediction of climate change and its impact on the northern cryosphere, especially hydrological systems, is a sound justification for monitoring lake ice dynamics. Climate change indicators based on lake ice phenology observations can contribute to better evaluation of potential effects and to identify mitigation and adaptation options. Thus, lake ice phenology is recognized and established as a tangible and technically feasible indicator of local climate change; it is used to support climate change research at all scales from local to global. For example the Canadian Council of Ministers of Environment (CCME) have established river and lake ice as one of 12 indicators of Canada's Changing Climate Indicators Initiative (http://www.ccme.ca).

Despite recognizing the importance of lake ice monitoring, observations of lake ice freeze-up, break-up and ice thickness have dramatically declined in Canada from 1980 to present (Lenormand et al., 2002). The number of monitored lakes has severely decreased, with few observations for northern lakes, and temporal gaps in existing records which reduce database utility. Costs involved in making observations as well as safety concerns for observers are suggested for the reduction (Lenormand et al., 2002).

Satellite remote sensing provides an alternative means to collect observations. A comprehensive overview on remote sensing methods, systems and applications for lake and river ice monitoring is presented in Jeffreis et al. (2005). Different remote sensing systems and information extraction techniques have been used to obtain ice freeze-up and break-up timing. Optical sensors with medium spatial resolution such as the Defense Meteorological Satellite Program Operational Linescan System (DMSP OLS, 0.55 km and 2.7 km spatial resolutions), Geostationary Operational Environmental Satellite Visible Infrared Spin-Scan Radiometer (GOES-VISSR, 1 km and 4 km spatial resolutions), Advanced High Resolution Radiometer (AVHRR, 1 km and 4 km spatial resolutions), and Moderate Resolution Imaging Spectrometer (MODIS; 250 m, 500 m, and 1 km spatial resolutions) have been used to estimate ice break-up based largely on visual image interpretation (Maslanik & Barry, 1987; Wynne & Lillesand, 1993; Wynne et al., 1996; Wynne et al., 1998; Pavelsky & Smith, 2004). Reported accuracies have ranged from 1.75 to 3.2 days. Microwave sensors with coarser spatial resolution data such as the Special Sensor Microwave Imager (SSM/I) with 25 km resolution have been used for mapping ice extent over seas and large lakes (Walker & Davey, 1993). Other efforts to monitor lake ice dynamics with active sensors include synthetic aperture radar (SAR), where much of the current research has focused on the use of radar measurements for ice thickness, break-up and freeze-up events (Jeffreis et al., 1994; Morris et al., 1995; Duguay & Lafleur, 1997; Duguay et al., 2002; Nolan et al., 2002; Duguay & Lafleur, 2003). Results are encouraging, but the temporal frequency (5–6 days) of current radar sensors and the short period for which measurements are available limits their use for climate change studies and operational monitoring. Break-up date detection can also be difficult with radar imagery when the surface is wet or contains pooling water (Hall et al., 1994). An example of an operational remote sensing application is weekly monitoring of ice extents for large lakes by the Canadian Ice Service (CIS). Since 1995 the CIS has been monitoring 136 lakes based on visual interpretation of NOAA/AVHRR and RADARSAT imagery with a reported accuracy ±1 week (Lenormand et al., 2002).

Medium resolution (0.25–1 km) optical satellite sensors such as the AVHRR, SPOT/VEGETATION, and MODIS provide daily global snow and ice coverage (Hall, 1998; Klein et al., 2000) thus ensuring the means to monitor spatial and temporal variability in snow/ice cover over large areas. The AVHRR sensors have the longest data record available from 1979 to present. Future MetOp missions planned as a collaborative effort between the U.S. and the European Space Agency will provide AVHRR data at least until 2020, ensuring 40 years of observations. However, to date remote sensing efforts for lake ice monitoring have only extended a few years and over small spatial extents (Jeffreis et al., 2005). Reasons for this underutilization are due to specific requirements for handling very large data sets, (magnitude of terabytes), consistent data preprocessing and lack of automated procedures for reliable information extraction.

In this study, the objective was to advance the use of historical long-term satellite data records for deriving lake ice phenology based indicators in support of climate change studies. Unlike the previous studies that utilize image interpretation to deduce lake ice phenology, an automated temporal profile technique for inferring ice phenology events from satellite records is presented and a comprehensive comparison with in-situ measurements is conducted. Results are used to extend the existing in-situ data record for trend analysis of 36 lakes. Satellite based records are also developed for 6 lakes in Canada's far north, for which no previous record existed and trends evaluated. Accordingly, the study is organized in the following three sections: i) information extraction for lake ice phenology from satellite observations; ii) evaluation of uncertainty of extracted information from satellite measurements against in-situ observations; and iii) trend analysis for Canadian lakes with available in-situ data.

2. Data and methods

2.1. Selected lakes

Lakes greater than 100 km^2 were extracted from the National Lake Cover Map of Canada (Davidson et al., 2006). In total 555 lakes had an area larger than 100 km^2, of which only 36 had sufficient in-situ data for trend analysis. Six lakes were selected to represent Canada's far north for which only satellite observations were available. For very large lakes only the area of the lake that was considered close to the ground observation point was extracted (i.e. within 50 km), islands were removed and lakes gridded to 1 km pixel size in order to spatially coincide with satellite data. A 3×3 erosion filter was applied to remove all edge pixels (i.e. pixels along shorelines). Fig. 1 shows the geographical location of the lakes analyzed.

2.2. Satellite data

A newly developed archive of ~ 1 km AVHRR image composites was used in the analysis. The data archive and products were assembled at the Canadian Center for Remote Sensing to support climate change studies over Canada. Overall ~ 350,000 orbits acquired with the series of National Oceanographic Atmospheric Administration satellites (NOAA 06–NOAA 17) were used to assemble 7000 single-day and 720 ten-day composites over Canada for the period from 1985 to 2004 (20 years). More information on the TIROS-N, NOAA-6 to NOAA-14 orbital and spacecraft characteristics, instruments and L1B data format is provided in NOAA Polar Orbiter Data User's Guide http://www2.ncdc.noaa.gov/docs/podug/ and http://www2.ncdc.noaa.gov/docs/klm/ for NOAA KLM satellites. Satellite data were processed with an improved methodology for georeferencing, sensor calibration, correction for viewing and illumination conditions (Latifovic et al., 2003), cloud screening (Khlopenkov & Trishchenko, accepted for publication) and advanced atmospheric correction.

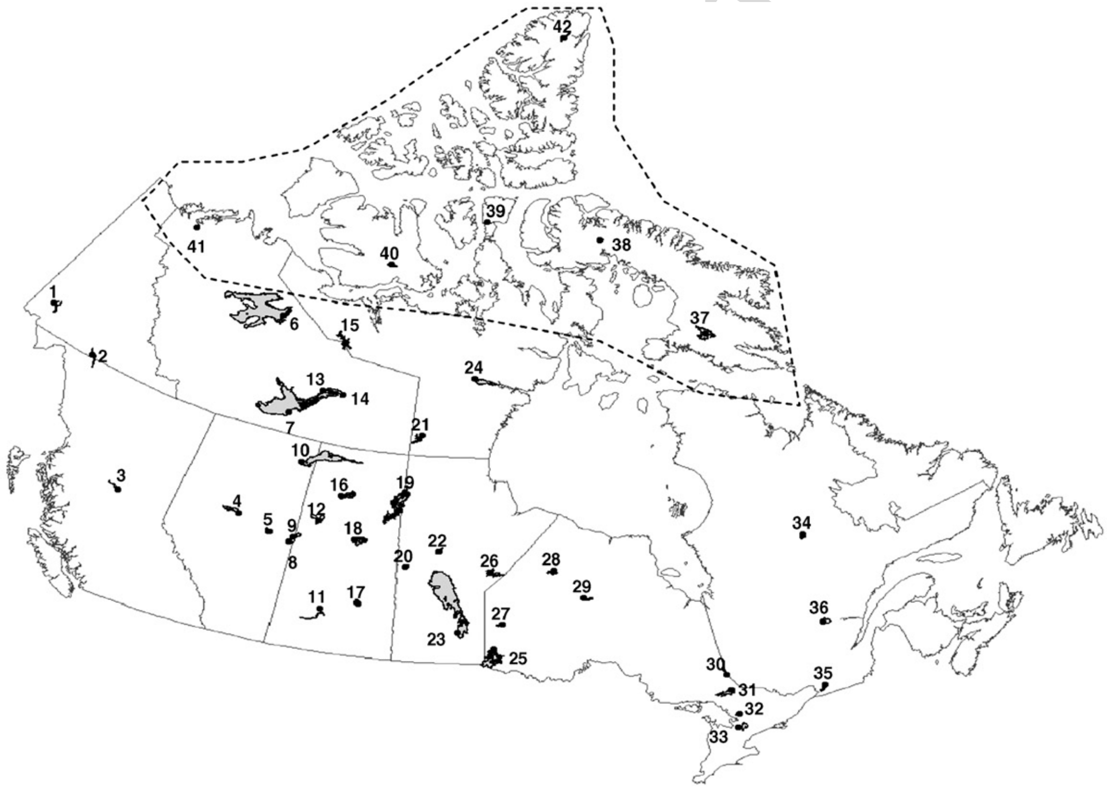

1. Kluane Lake	8. Cold Lake	15. Contwoyto Lake	22. Setting Lake	29. Attawapiskat Lake	36. Lac St. Jean
2. Teslin Lake	9. Primrose Lake	16. Cree Lake	23. Lake Winnipeg	30. Lake Temiskimang	37. Amadjuak Lake
3. Stuart Lake	10. Lake Athabasca	17. Big Quill Lake	24. Baker Laker	31. Lake Nipissing	38. Angajurjualuk Lake
4. Lesser Slave Lake	11. Diefenbaker Lake	18. Lac La Ronge	25. Lake of the Woods	32. Lake Muskoka	39. Stanwell-Fletcher Lake
5. Lac La Biche	12. Churchill Lake	19. Reindeer Lake	26. Island Lake	33. Lake Simco	40. Washburn Lake
6. Great Bear Lake	13. Great Slave Lake - Charleton Bay	20. Clearwater Lake	27. Red Lake	34. Nitchequon Lake	41. Sitidgi Lake
7. Great Slave Lake - Resolution Bay	14. Great Slave Lake - Mcleod Bay	21. Ennadai Lake	28. Big Trout Lake	35. Lake St. Louis	42. Lake Hazen

Fig. 1. Names and locations for lakes analyzed. Dashed line identifies lakes in the far north for which only a 20 year remote sensing record was available.

The baseline data covers an area of 5700 km East–West by 4800 km North–South or 5700 pixels by 4800 lines at a spatial resolution of 1 km. The established grid system is based on the ellipsoidal version of the Lambert Conformal Conic (LCC) projection as defined by the NAD83 datum. The central meridian at 95° W, latitude of origin at 0° N and the standard parallels set at 49° N and 77° N. It is important to highlight that before geometric corrections, the pixel ground resolution ranges from 1.1 km at nadir to 5 km (along track) by 6.8 km (across track) at the scanning extreme of 55.4°. The geocoded images have had geometric corrections applied so that the size for all pixels is nominally 1 km^2. However, the quality decreases further from the nadir view. To reduce this effect, pixels closer to nadir were favored in assembling the daily composites. A full description of the processing system, satellite data archive and image products are provided in Latifovic et al. (2005).

Average daily reflectance measurements in the visible, near-infrared, and thermal wavelengths as well as a cloudiness index were extracted over all 555 lakes for the period from 1985 to 2004. It is important to emphasize that most of the publicly available composite data (AVHRR Pathfinder, MODIS, SPOT/VGT S10) are based on maximal vegetation index criteria that generate data suitable for land related applications, but cannot be used for water bodies as this criteria preferentially selects clouds over water. For this study single day composites were assembled using minimal visible reflectance criteria which is more appropriate for selecting clear sky observations over water.

The other available AVHRR time series with comparable spatial resolution is AVHRR Polar Pathfinder Twice-Daily 1.25 km EASE-Grid Composites (Scambos et al., 2000), but has shorter temporal coverage from August 1993 through December 1998.

2.3. In-situ lake ice phenology data

Two sources of in-situ data were used. The majority were from the Canadian Ice Database (CID) developed by Lenormand et al. (2002). Four southern lakes were taken from the Global Lake and River Ice Phenology Database (GLRID) (Benson & Magnuson, 2000). The CID contains records covering the period 1822–2001, but with a significant decrease in the observation-network for the period from 1985 to 2004 that overlapped the satellite data record.

2.4. Lake reflectance temporal profile

The conventional visual image interpretation approach to extract lake ice phenology events for a long period involves significant time and resource commitments. To overcome this problem an extraction technique was devised that uses the reflectance temporal profile as a convenient way to manipulate and automatically extract the ice events of interest. The use of profiles dramatically reduces the data volume, by replacing the series of satellite images with a single file that contains only the needed lake observations. An example of a lake reflectance temporal profile assembled from AVHRR daily observations is illustrated in Fig. 2 along with example images of the ice events. Every point represents the top of atmosphere reflectance averaged over all the pixels within the lake. Ordered by time, the observations render the lake spectral development through the season in the visible or near infrared wavelengths (Fig. 2 shows near infrared). Near infrared is preferred because it is not as heavily influenced by atmospheric conditions compared to red wavelengths. The yearly thermal cycle for the lake is also shown in Fig. 2 based on brightness temperature (BT) computed from AVHRR thermal band observations. The lake ice phenology is characterized with the following four events in the profile: 1) ice break-up start (BUS), 2) ice break-up end (BUE), 3) freeze-up start (FUS) and 4) freeze-up end (FUE). The slope of the line connecting BUS and BUE determines the rate of ice melt, which depends on the amount of ice, climate conditions and radiation energy. Time between FUE and BUS determines the ice-on duration, while time between BUE and FUS determine ice-off duration. The BUS and BUE events, as determined from the reflectance profiles, generally coincide with the BT profile points. The beginning of break-up is indicated by cooler (negative) temperatures approaching zero and break-up completion occurs at a temperature of around 4 °C. Thus the BT profile could be used as an additional source of information for extracting ice phenology events. It also provides seasonal lake temperature dynamics which influences all aspects of the lake system. However, for this study only the optical measurements were used to infer ice phenology to minimize overall processing requirements.

2.5. Profile feature extraction

The temporal profile in Fig. 2 shows high variability in observed lake ice reflectance making accurate feature extraction a relatively difficult task. The major source of variability in reflectance measurements are different atmospheric conditions during acquisition, the presence of clouds and haze, cloud shadows, and unfavorable illumination conditions and viewing geometry, especially for northern lakes where sun elevation in winter is very low. In addition to scene acquisition conditions, ice and snow reflective properties also change as a function of surface roughness, near-surface liquid water content, snow age and the presence of impurities (Wynne & Lillesand, 1993). Therefore, the first step for successful feature extraction is noise reduction. This is usually performed through filtering outliers to produce a stable temporal profile that is more indicative of the attributes to be extracted. In this approach, a morphological filtering method was used where a lake specific template profile was applied to the data set in order to remove outliers. The template profile was derived for each lake, consisting of the average and 95% lower and upper bounds (i.e. 1.96 standard deviations from the mean) computed within a moving window interval (e.g. 10 days) for several years (e.g. 10). All observations outside the template envelope were removed from further analysis. For the final step of the extraction, two approaches were considered i) extraction through profile visual interpretation and ii) automated extraction based on reflectance thresholds. Both methods were evaluated to determine if the automated

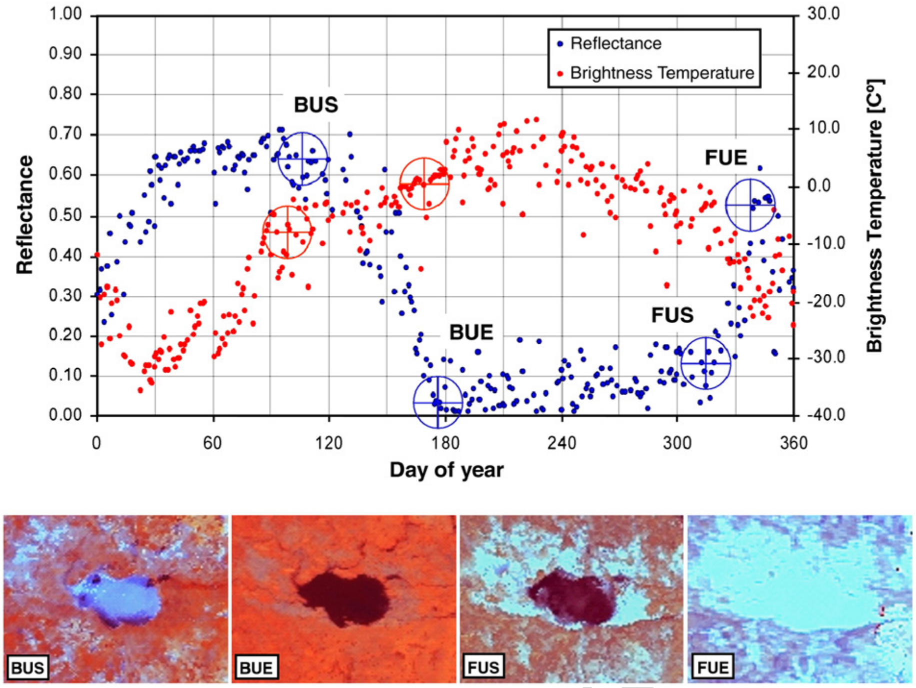

Fig. 2. Lake ice phenology profile assembled from AVHRR daily observations and sample imagery displayed as red — normalized vegetation index, green — near infrared, and blue–red. Acronyms denote start of ice break-up (BUS), end of ice break-up (BUE), start of freeze-up (FUS), and end of freeze-up (FUE).

method could achieve acceptable results to allow processing of a large number of lakes.

2.5.1. Visual extraction

The visual extraction of phenology events was based on the comparison between a simplified profile shape (Fig. 3) and the actual lake reflectance profile. In the simplified profile shape ice reflectance between FUE and BUS, and water reflectance between BUE and FUS are assumed as constant values while periods of melting and freezing are indicated by constant slope lines. The task for the interpreter was to visually adjust the simplified profile to fit the actual profile points in order to decide where intersections among these lines were. An exception was for FUE, where due to a large amount of missing satellite observations during this event, the most robust approach was found to be the use of a simple reflectance threshold of 0.5.

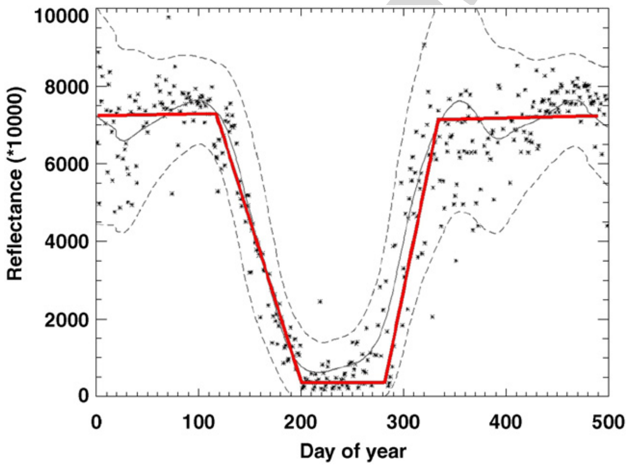

Fig. 3. Example lake reflectance temporal profile for extracting phenology dates. Thin grey line shows mean, upper and lower dashed lines shows 95% bounds, red line shows simplified profile.

2.5.2. Automated extraction

The general processing steps for the automated procedure are depicted in Fig. 4. The first step is the same as that discussed previously for outlier removal from the reflectance profile.

After filtering, gaps in the profile were filled using the linear interpolation of neighboring values. Two curves were fit to the data for the upper and lower bound. The lower bound fit was used to extract features that exist in the lower portion of the reflectance profile (i.e. BUE and FUS), where errors due to bright artifacts (e.g. cloud and haze) would have a much greater influence than dark artifacts (e.g. shadow). For features in the brighter portion of the profile (i.e. BUS and FUE) this would be the opposite and thus the upper bound fit was used to exact these features.

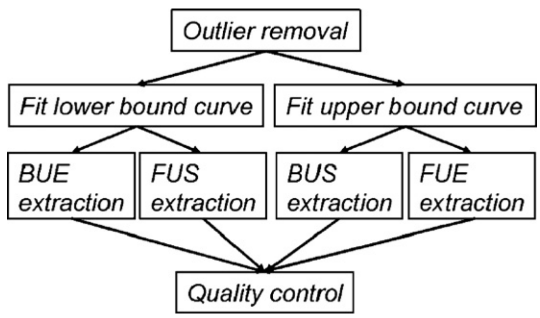

Fig. 4. Flowchart of the automated extraction procedure.

To determine the lower bound curve, the maximum of minimum values in a split moving window was used. The window size was set at 16 days, split equally into two 8 day sub windows. For the upper bound, the minimum of maximums was used with the same moving window sizes. After filtering, the curves contained considerable undesirable fine-scale variability. To remove this, Lowess smoothing was applied. Lowess smoothing performs a locally weighted linear regression to determine the smoothed value at each point based on a defined window size (Mathworks, 2006). For the lower bound curve, extracted features (i.e. BUE and FUS) were generally associated with a more rapid change in the reflectance profile than those for the upper bound curve (i.e. BUS and FUE). Thus, to preserve these features in the lower bound curve, Lowess smoothing was applied with a smaller window size (i.e. less smoothing). For the lower bound curve the window size was set at 11 days and 21 days was used for the upper bound curve. These parameters were identified through sensitivity analysis of a subset of lakes distributed from north to south.

The extraction of phenology events from each profile was based on two iterations, where in the first iteration a reflectance threshold was used to estimate an initial position for a phenology event. As the threshold was defined to be suitable for the majority of lakes in Canada it resulted in event positions being estimated slightly earlier than the correct position. Thus, in the second iteration, the result of the first iteration was used to sample neighboring values to define a new threshold that better represented the specific properties of the profile being processed. For BUS, BUE, and FUS two conditions were assessed for selection of the event position. FUE was not processed with the second condition due to a high proportion of missing data around the time of the FUE event for some lakes and for certain years. The first condition was a spectral threshold (Eq. (2)), where the majority of the data in a profile sample window was required to be above or below a threshold value. The second condition (Eq. (3)) evaluated whether the position was plausible based on a loosely defined expected morphology profile. For lakes, phenology events occurred close to distinct points of high curvature in the profile. Thus testing the rate of change around a potential position provided a secondary check on the suitability of the extracted position.

Specifically for a given profile sample window defined as:

$$S(i-n,\ i-n+1, \ldots i+n) \tag{1}$$

where i denotes position in days, $2n+1$ is the sample window size, and S is the reflectance value at position i. In this analysis the sample window size used was 9 days (i.e. $n=4$). The two threshold conditions were calculated as:

$$T_1 = \frac{1}{2n+1}\sum_{i=i-n}^{i=i+n} D_i; \quad D_i = \begin{cases} S_i<t = 1 \\ S_i>t = 0 \end{cases} \tag{2}$$

$$T_2 = M_1/M_2; \quad M_1 = \frac{1}{T_1(2n+1)}\sum_{i=i-n}^{i=i+n} S_i D_i; \tag{3}$$

$$M_2 = \frac{1}{2n+1}\sum_{j=i+10-n}^{j=i+10+n} S_j$$

where t is the initial reflectance threshold for the phenology event to be extracted, T_1 is the percentage of values in the first sample window below t, T_2 is the ratio between the mean in the first and second sample windows, M_1 and M_2 respectively. M_1 is calculated only for values meeting the threshold condition and M_2 is simply the mean in a 10 day window positioned 10 days from the M_1 window. In the second iteration the reflectance threshold value t is defined based on the mean for the 10 days following the point found in the first iteration. Specific criteria used for event detection were:

BUS = position i where $T_1 \geq 0.7$ and $T_2 \geq 1.4$ and $S_i \geq t$ for $t=0.6$.
BUE = position i where $T_1 \geq 0.7$ and $T_2 \leq 1.4$ and $S_i \leq t$ for $t=0.08$.
FUS = position i where $T_1 \leq 0.3$ and $T_2 \geq 0.4$ and $Si \geq t$ for $t=0.08$.
FUE = position i where $T_1 \leq 0.3$ and $S_i \geq t$ for $t=0.5$.

A lower initial threshold (t) was used for FUE compared to BUS to offset the influence of lower sun elevation during this time making the reflectance of ice darker.

The final step in the automated processing was to check for unlikely estimates. This was accomplished by converting the estimates for each lake to z-scores and graphing these to identify outliers. Any potential outliers were checked by visual evaluation of the profiles and corrected if automated extraction appeared to have failed. For FUE, 16% of the events had to be checked and 11% replaced with visual interpretation. In extracting BUE events the automated procedure performed much better and only 6% required checking and 4% of them required replacement with visual interpretation.

2.6. Comparison with in-situ data

Agreements between in-situ and remote sensing phenology event estimates were measured by the mean absolute error (MAE) and r^2. Trends were determined based on Sen's median of slopes method (Sen, 1968). In total 20 lakes had sufficient data for validation of satellite derived ice event estimates.

2.7. Trend analysis

The magnitude of the trend was assessed following Sen (1968). Trend significance was evaluated using the statistical rank-based non-parametric Mann–Kendall test (Mann, 1945; Kendall, 1975). This approach to trend assessment is commonly used in hydrological research (Yue et al., 2002). A correction for autocorrelation was also applied following the approach proposed in Yue et al. (2003). Trends for 36 lakes were calculated using the combined in-situ and remote sensing observations for the complete data record and for the period 1970–2005. Only BUE and FUE were assessed for trends because 1) these events had the highest agreement between in-situ and satellite estimates, 2) considerable in-situ data was available for both events, 3) together they represent the ice off duration, and 4) these the are the measures commonly used in other studies.

Of the two measures much of the effort was focused on the analysis of BUE because the results of the in-situ comparison revealed that it was the most accurately estimated phenological event from remote sensing.

To align (i.e. calibrate) the remote sensing and in-situ data it was determined that a lake specific correction was required to reduce the potential for biasing trends. This was done in two ways depending on the nature of the overlap between the two data sources. If at least 5 years of observations overlapped between the in-situ and remote sensing data then the mean bias between these observations was used for correction. In the case where no overlap existed and the gap between observations was less than 10 years, the difference between the mean for the last 5 years of the in-situ data and first 5 years of the remote sensing data was used. This approach is unlikely to generate false trends and more likely to reduce the ability to identify significance trends. Thus trend estimates for lakes that this calibration method was used are considered conservative.

Data used in the trend analysis was based on the automated extraction, as the comparison with in-situ data revealed that it produced similar results to visual extraction and drastically reduced the time required for processing. However, in the far north the profiles were more variable with years where the lake did not break-up or a large section of ice remained within the lake throughout the year. Thus, visual extraction was used for northern lakes. In years where the lake did not break-up the latest date observed for break-up of the lake in the 20-year record was used in order to derive an estimate of the trend

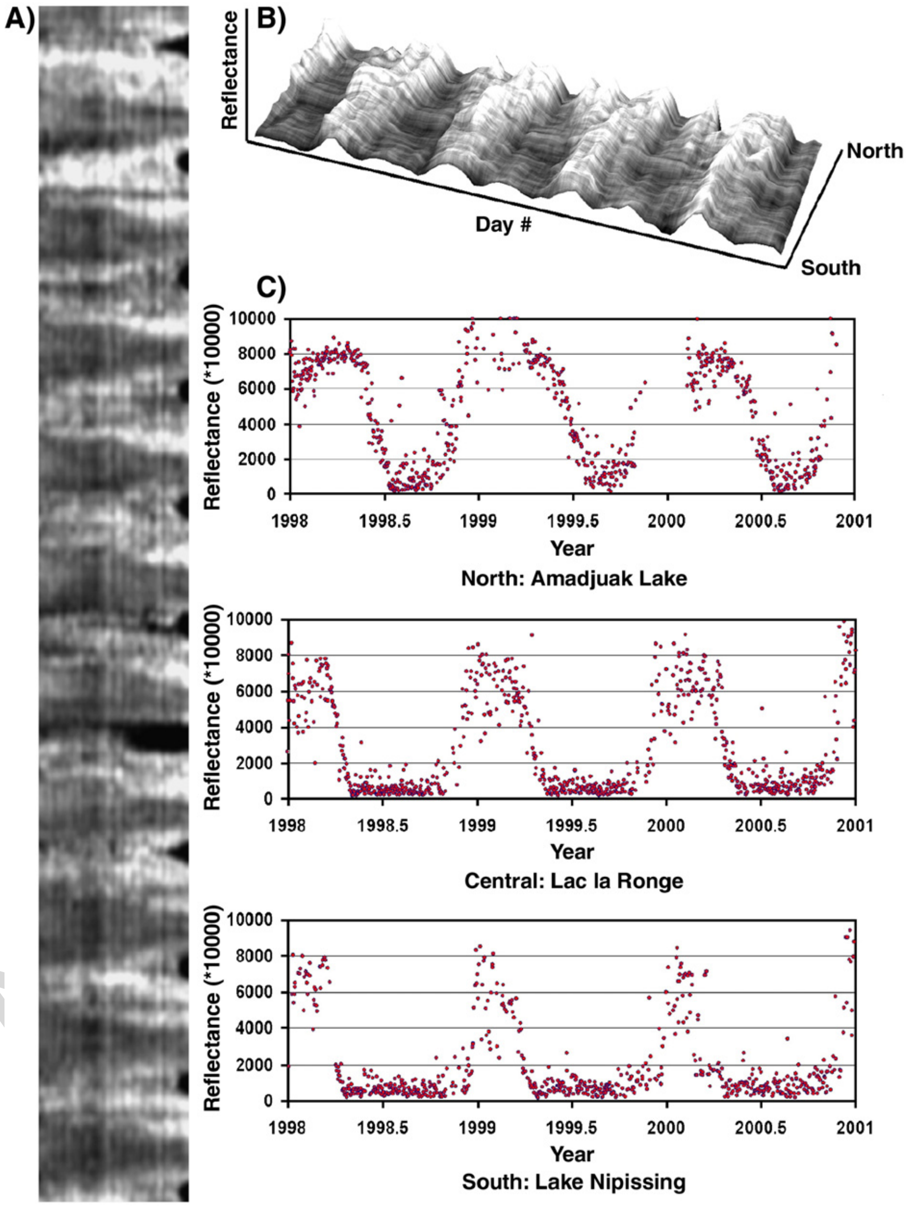

Fig. 5. Visualization of profile data. A) Shows a sample section of the matrix from 1994–2004 where brighter values represent ice snow and darker values water, black areas are gaps of missing data in the time series. The duration of ice off conditions is clearly identifiable in the image, with the longest duration in the south (right) and shortest in the north (left). B) Three dimensional view of the matrix. C) Example profiles for three lakes representing a gradient from north to south.

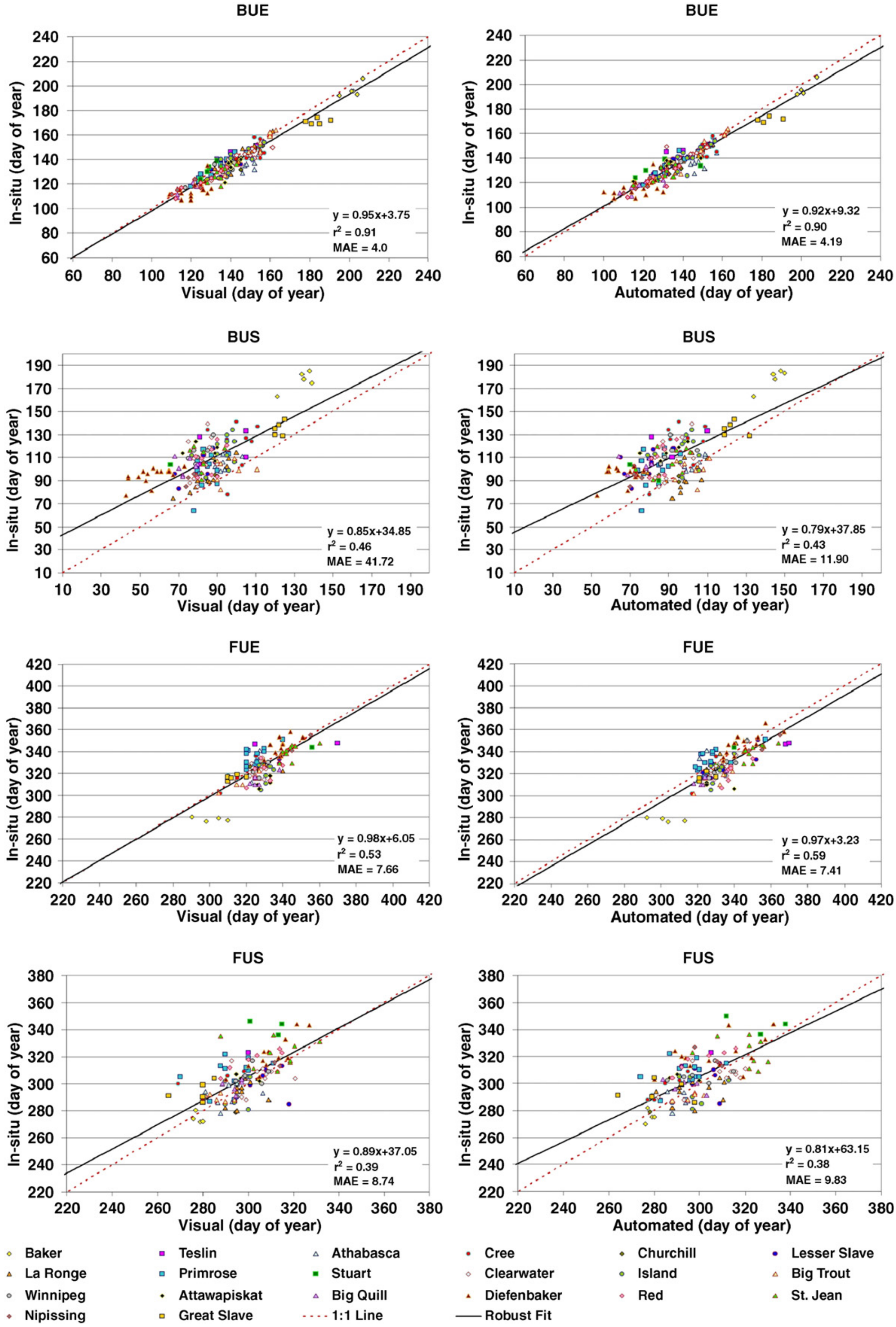

Fig. 6. Results of comparison between phenology dates obtained from ground observations and satellite remote sensing. Right shows comparison for visual assessment and left shows comparison for automated analysis.

magnitude and significance. Of the 6 lakes analyzed, the two furthest north (Stanwell–Fletcher and Hazen) did not completely break-up in all years. Lake Hazen did not break-up in 1985–1987, 1992, 1996, and 2004. Stanwell–Fletcher did not break-up in 1986, 1990, 1992, and 2004.

3. Results and discussion

3.1. Data quality and visualization

AVHRR red and near infrared reflectance profiles were extracted for 555 lakes for the period 1985 to 2004. Results were stored as a matrix $[M]$ (i, j, k) where $i=555$ number of lakes, $j=7300$ number of days and $k=2$ number of spectral bands. A sample section of the matrix from 1994–2004 is shown as an image in Fig. 5a where lake profiles were ordered by latitude, south to north, from the left side to the right side of the image. This form of combining lake profiles into a single dataset is a convenient way to store, visualize (Fig. 5b) and assess data quality. Several data gaps (black areas on right of Fig. 5a) are caused by very low solar elevation during winter. These gaps are present during the first 3 months of the year and their duration depends on lake latitude. There is also somewhat lower data quality at the beginning of the record (1985–1989) because the available number of orbit segments for assembling single day composites in these years was only 5% of the average number of orbits available in other years.

Fig. 5a shows the general change in ice-water proportions along the south-north gradient (bright regions in the image represent ice/snow while darker regions represent water). Fig. 5c shows the reflectance profiles of three lakes geographically located in the southern, central boreal and northern regions of Canada. Climate-specific lake ice phenology is well captured by the reflectance profiles. For the northern lake ice-off duration is on average 60 days, 2.8 times shorter than the lake in the central boreal region and 3.5 times shorter than the lake in the southern region. Differences in the rate of melting and freezing defined by the slope of the transition period are in general agreement with the lakes' regional climate conditions. These characteristic examples are provided to demonstrate the feasibility of long-term satellite data records to capture regional phenology differences.

3.2. Comparison with in-situ data

The comparison results with in-situ data are shown in Fig. 6 for the different phenology events. Results for both the visual and automated extraction are quite similar with slightly lower MAE and higher r^2 for three of the four events with the visual results. Agreement between the visual and automated estimates was high with $r^2>0.9$.

BUE showed the strongest agreement with no apparent systematic or lake specific bias. The strong agreement, to some extent, can be explained by the clear BUE event definition as the time when water is completely free of floating ice. This change in lake conditions is associated with a strong difference in reflectivity that can be easily detected in satellite observations and occurs during the time of year with a relatively high sun elevation making observations the most consistent. The mean absolute error of 4.2 days is a good result considering that ice break-up is not an abrupt event and requires observer judgment, thus a part of the uncertainty perhaps can be assigned to the in-situ observations.

FUE showed the next best agreement with a MAE of 7.4 days. Some lakes showed specific biases evident as points departing to one side of the robust fit line (i.e. Baker lake and Primrose lake). This suggests either a consistent error in the extraction procedure specific to these lakes or differences in how in-situ observations are made between lakes.

Evaluation of BUS events showed a MAE of 11.9 days and persistent underestimation of satellite observations compared to in-situ observations. The bias is likely the result of changes in lake snow/ice reflectivity (e.g. water content, surface roughness, and presence of impurities) that are more readily detected by remote sensing indicating the initiation of melt. This bias is largely systematic, but some specific lake deviations were evident.

FUS had the poorest linear relation, with the second highest MAE of 9.8 days and systematic underestimation of in-situ

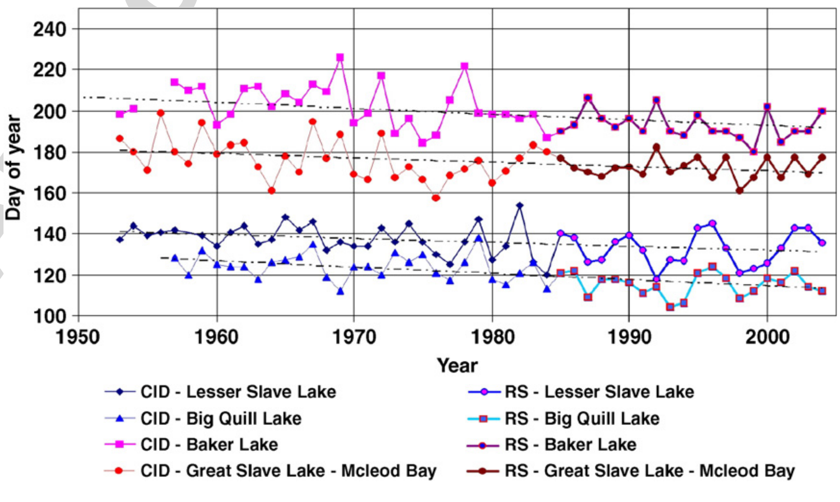

Fig. 7. Trend of ice break-up timing for four Canadian lakes, spatially distributed from south to north.

points. This result is somewhat surprising as FUS appeared to be a distinct feature in the reflectance profiles for the majority of lakes examined. It is possible that the in-situ definition of first ice varies between lakes and could explain these results. Also, ice formation is dynamic and can form and melt quickly during this period, which could also have contributed to this result.

The agreements between in-situ and lake ice phenology data extracted from satellite records were also evaluated through analysis of trend continuity. Fig. 7 shows an example BUE time series for four lakes spatially distributed from south to north in west-central Canada. The period from 1954 to 1984 are in-situ observations and from 1985 to 2004 were extracted from remote sensing data. In all four cases remote sensing observed BUE dates show a similar trend as determined for the period when only in-situ observations were available, clearly supporting the assumption that remote sensing can be combined with ground observations for obtaining a more complete record. Fig. 7 also shows that geographically closer lakes, in this case Lesser Slave Lake and Big Quill Lake in the south; and Great Slave Lake and Baker Lake in the north are under similar local climate conditions and thus exhibit comparable inter-annual variability. This similarity is more pronounced in the part of the record based on remote sensing observations underlining its consistency.

Table 1
Trends in BUE from combined in-situ and remote sensing observations

Name	Complete record			1970–2004			In-situ	
	Slope	*Z*-Score	Cases	Slope	*Z*-Score	Cases	First Measured	Last Measured
Kluane Lake	−0.239	−1.283	37	−0.267	−1.440	34	1967	1984
Teslin Lake	**−0.272**	**−3.414**	**54**	**−0.333**	**−1.807**	**35**	1949	1989
Stuart Lake*	−0.107	0.100	28	−0.286	−0.787	30	1975	1989
Lesser Slave Lake*	**−0.229**	**−2.197**	**51**	−0.100	−0.114	35	1953	1993
Lac la Biche	**−0.131**	**−1.743**	**53**	−0.290	−1.209	31	1946	1980
Great Bear Lake	**−0.222**	**−1.986**	**33**	−0.267	−0.984	25	1954	1974
Great Slave Lake – Resolution Bay	**−0.333**	**−2.379**	**37**	−0.050	−0.099	28	1957	1977
Cold Lake	**−0.190**	**−2.317**	**62**	−0.283	0.889	35	1941	1989
Primrose Lake*	−0.250	−1.188	39	**−0.429**	**−1.764**	**35**	1962	1999
Lake Athabasca*	−0.270	0.387	40	−0.600	1.007	34	1963	1994
Lake Diefenbaker*	−0.200	−0.637	33	−0.469	− 1.536	35	1969	1999
Churchill Lake	0.077	0.078	33	−0.211	−0.435	33	1969	1993
Great Slave Lake – Charleton Bay*	−0.167	0.105	43	0.227	1.396	35	1957	1989
Great Slave Lake – McLeod Bay	**−0.273**	**−2.153**	**47**	0.105	0.314	35	1953	1986
Contwoyto Lake	−0.052	0.045	34	0.050	0.552	32	1968	1981
Cree Lake*	−0.083	−0.128	35	−0.083	−0.128	35	1970	1993
Big Quill Lake*	**−0.385**	**−4.159**	**48**	**−0.500**	**−3.332**	**35**	1957	1991
Lac la Ronge*	0.074	0.176	38	0.118	0.270	35	1967	1997
Reindeer Lake	**−0.224**	**−3.104**	**52**	−0.133	−0.661	30	1947	1980
Clearwater Lake*	−0.118	−0.450	47	−0.179	−0.469	35	1959	1996
Ennadai Lake	**−0.286**	**−2.361**	**44**	0.222	0.931	30	1955	1979
Setting Lake	−0.050	−0.237	34	−0.200	−0.272	21	1957	1970
Lake Winnipeg*	−0.109	−1.048	58	−0.300	−1.493	35	1947	1990
Baker Lake*	**−0.389**	**−3.406**	**51**	**−0.303**	**−1.735**	**35**	1953	1990
Lake of the Woods	**−0.400**	**−3.897**	**43**	**−0.500**	**−2.326**	**33**	1956	1990
Island Lake*	−0.400	−1.514	34	−0.400	−1.514	34	1971	1998
Red Lake*	**−0.227**	**−1.854**	**44**	**−0.342**	**−1.906**	**35**	1957	1992
Big Trout Lake*	**−0.231**	**−2.168**	**55**	−0.200	−0.782	35	1947	1990
Attawapiskat Lake*	**−0.419**	**−4.246**	**53**	**−0.660**	**−3.469**	**35**	1949	1989
Lake Timiskaming*	−0.044	−0.610	105	−0.417	−0.650	20	1900	1995
Lake Nipissing	−0.106	−0.596	48	**−0.333**	**−1.920**	**35**	1957	1988
Lake Muskoka*	−0.015	−0.122	105	−0.133	−0.597	35	1900	1994
Lake Simcoe*	−0.051	−0.777	92	−0.197	−0.554	35	1901	1995
Lac Nitchequon	−0.125	−0.906	53	−0.107	−0.185	35	1947	1985
Lac Saint-Louis	−0.124	−0.859	43	−0.306	−1.463	31	1957	1981
Lac Saint-Jean*	0.077	0.806	53	−0.125	−0.238	34	1942	1997
Far North								
Amadjuak Lake	−1.000	−1.569	20					
Angajurjualuk Lake	−0.750	−0.196	20					
Stanwell–Fletcher Lake	−0.200	−0.221	20					
Washburn Lake	−0.600	−0.457	20					
Sitidgi Lake	−0.571	−1.453	20					
Lake Hazen	**−2.875**	**−2.385**	**20**					

An * indicates lakes that that were calibrated using overlapping data.
Bold identifies lakes that were significant at the 90% confidence interval.

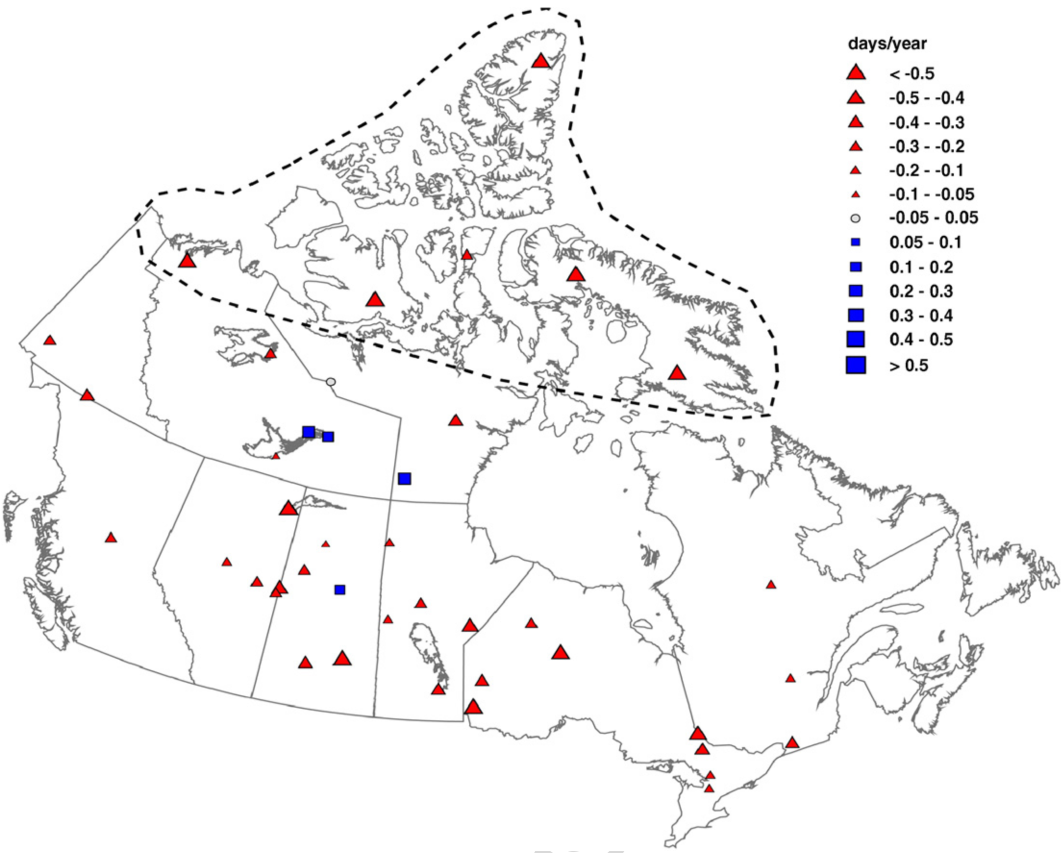

Fig. 8. Spatial pattern of break-up trends for the period 1970–2005. Dashed line identifies lakes in the far north for which only a 20 year remote sensing record was available.

3.3. Trend analysis

3.3.1. Break-up

Table 1 provides BUE trend statistics and Fig. 8 shows a spatial representation of these results for the period 1970–2004. For the complete record of 36 lakes with in-situ data 33 showed a trend towards earlier BUE and 15 were statistically significant at the 90% confidence level. The average rate of change in BUE was −0.18 days/year. For the period 1970–2004, slopes on average increased to −0.23 days/year, 31 of the lakes had a negative trend, and the number of significant lakes almost halved to 8. The increase in the slope magnitude is consistent with the temperature record, which shows the greatest increase occurring from 1970 onward (Hansen et al., 1999). The reduced

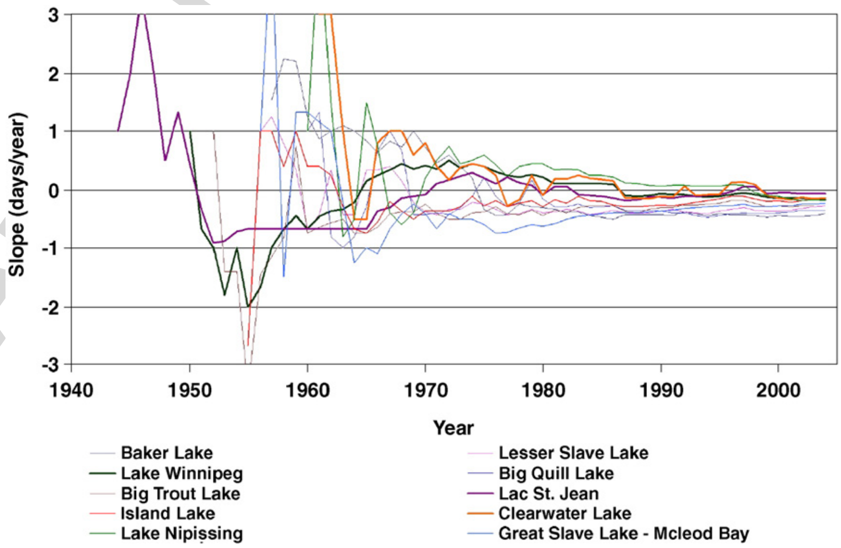

Fig. 9. Examples of trend slope variability with record length.

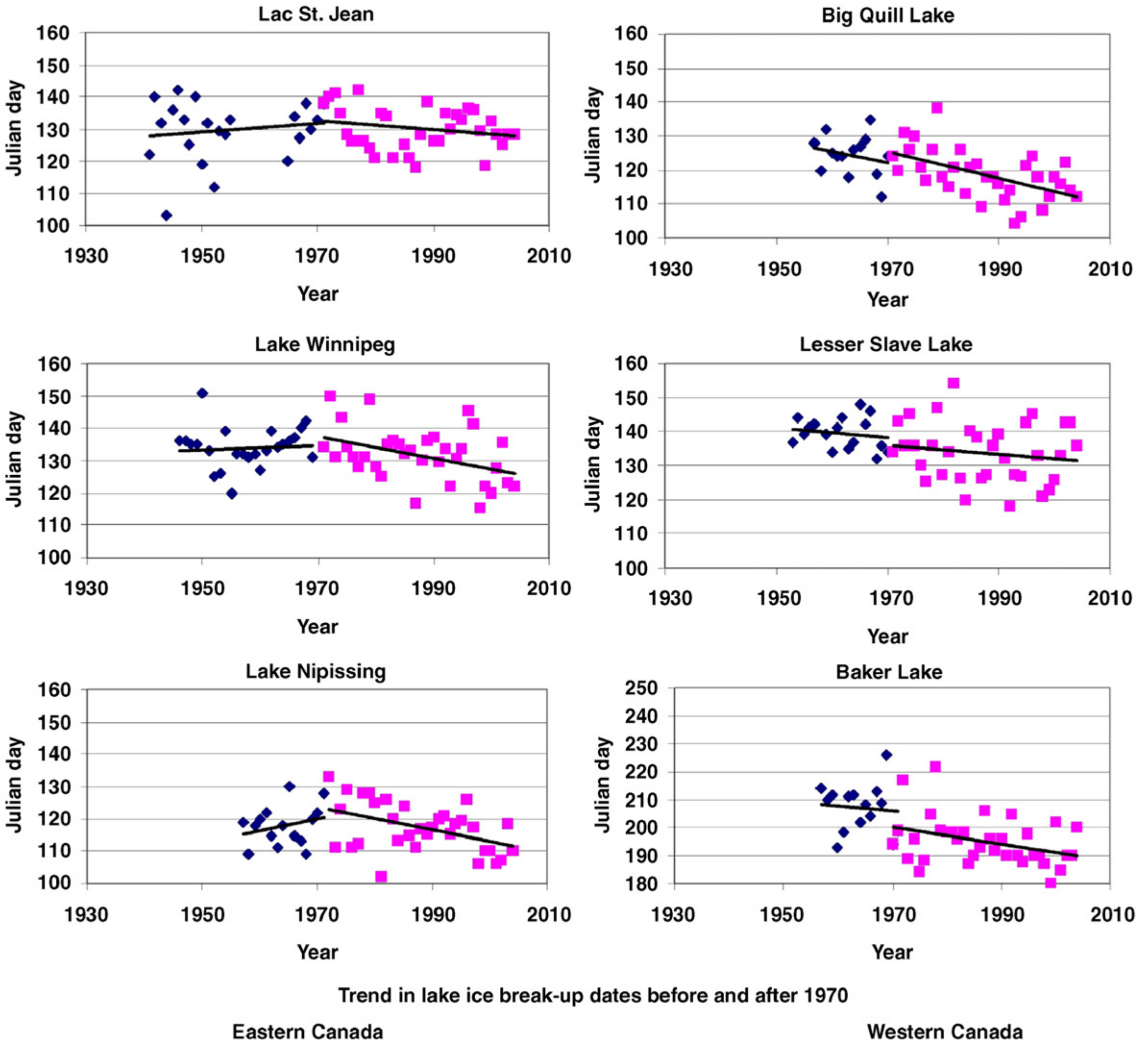

Fig. 10. Example of differences in trend morphology for lakes in Eastern and Western Canada.

number of significant trends was most likely the result of the shorter record length. Spatially, trends in BUE were considerably variable due to numerous factors known to affect ice formation and break-up other than temperature including winter precipitation; lake morphology (area, volume, depth); topography (influences local climate and shade dynamics); and water flow from input streams, rivers and surface flow (Jeffreis et al., 2005). In terms of trend magnitude, no specific regions were identifiable except a possible area of week trends in the east and moderate trends in the west. An area of later break-up is evident in the north-central region. Results reported by Duguay et al. (2006) for the period 1971–2000 using only in-situ observations appears to support this result, with 3 of the 4 lakes in the region having no trend or a trend towards later break-up dates. Temperature trends reported in Serreze et al. (2000) also appear to support these findings, showing an area of cooling in the north-central region and strongest temperature increases in the south-central to north-west region of Canada. Comparison of inter-annual variability for the period 1970–2004 to 1950–1970 supports the results identified by Magnuson et al. (2000). Of the 26 lakes for which the comparison could be made, 16 showed an increase in variability. It is important to note that this comparison was made using data that was not collected in the same manner and thus the increase could be the result of differences between the in-situ and remote sensing measurements.

Trends in BUE for the six lakes in the far north were analyzed using the 20 year remote sensing record because remote sensing was the only available data source. All lakes analyzed showed strong negative trends, but only one was statistically significant. The average change in BUE was considerably higher than the rest of Canada (−0.99 days/year). This finding supports other studies that have identified a climate warming influence on northern artic sea-ice, glaciers, permafrost and plant growth summarized in Serreze et al. (2000). However, due to the short record, further monitoring will be critical to more conclusively determine and quantify the magnitude of this trend.

With a longer time series it is expected that more trends would be found significant if the trend does not alter its direction, as one of the major factors found to affect significance of the Mann–Kendal test is time series length (Yue et al., 2002). To gain further insight into this influence, trend slope variability related to record length was analyzed by computing the trend for each year, using observations from all previous years. An example for several lakes is shown in Fig. 9. From Fig. 9 it is evident that the trend (i.e. slope) for these lakes becomes stable when the record includes at least 30 years of observations. For most of the examples presented, when the slope is relatively stable it exhibits small variations with amplitude of about 8 years.

The analysis of trend versus record length revealed different trend behaviors in the temporal and spatial domain. From 1970 the trends generally increase, but the change is most apparent for lakes in Eastern Canada (Table 1, Fig. 10). On average trends in Eastern Canada increased by a factor of 4 comparing the complete record to the period 1970–2004, whereas little change was found for Western Canada. However, due to the length of the available records it is not possible to determine if this is the influence of longer term climate variability in the eastern region, where the trend from 1970 may only be part of the downward aspect of a longer term cycle.

3.3.2. Freeze-up

Table 2 provides FUE trend statistics and Fig. 11 gives a spatial representation of these results for the period 1970–2004. Of the 36 lakes with in-situ data 24 showed a trend towards later FUE. Of these 10 were statistically significant at the 90% confidence level. The average rate of change in FUE was

Table 2
Trends in FUE from combined in-situ and remote sensing observations

Name	Complete Record			1970–2004			In-situ	
	Slope	*Z*-Score	Cases	Slope	*Z*-Score	Cases	First measured	Last measured
Kluane Lake	−0.261	−0.412	35	−0.207	−0.289	31	1966	1984
Teslin Lake	0.158	0.410	50	−0.073	−0.300	29	1949	1986
Stuart Lake	**0.843**	**1.870**	**25**	**1.000**	**2.671**	**23**	1974	1989
Lesser Slave Lake*	0.083	0.156	47	0.250	0.801	31	1953	1992
Lac la Biche	**0.283**	**3.260**	**50**	0.287	1.347	26	1944	1980
Great Bear Lake	0.052	−0.544	32	**−0.604**	**−2.066**	**22**	1952	1973
Great Slave Lake – Resolution Bay	−0.224	−1.423	36	**0.429**	**2.036**	**21**	1956	1976
Cold Lake	0.136	0.605	48	**0.480**	**2.286**	**30**	1952	1988
Primrose Lake*	0.182	0.608	41	0.333	0.714	29	1961	1999
Lake Athabasca*	0.218	1.283	37	0.051	0.097	32	1965	1993
Lake Diefenbaker*	**0.786**	**3.339**	**34**	**0.750**	**2.873**	**29**	1968	1998
Churchill Lake	**0.495**	**4.096**	**31**	**0.400**	**3.637**	**29**	1969	1987
Great Slave Lake – Charleton Bay	−0.036	−0.028	46	−0.200	−1.153	32	1956	1989
Great Slave Lake – McLeod Bay*	**0.408**	**3.383**	**42**	0.257	1.071	32	1953	1990
Contwoyto Lake	0.211	0.982	27	0.211	0.982	27	1970	1979
Cree Lake*	**−0.394**	**−1.721**	**34**	**−0.394**	**−1.721**	**34**	1970	1992
Big Quill Lake*	**−0.250**	**−1.797**	**48**	−0.180	−0.520	34	1956	1990
Lac la Ronge*	−0.190	−0.851	37	0.097	0.119	34	1967	1996
Reindeer Lake	0.055	0.142	50	0.176	0.641	26	1946	1979
Clearwater Lake*	0.080	0.062	48	0.176	0.594	34	1956	1996
Ennadai Lake	0.186	1.519	44	0.378	1.633	28	1955	1979
Setting Lake	0.104	0.465	33	0.667	1.263	19	1956	1970
Lake Winnipeg*	−0.091	−0.659	48	−0.133	−0.653	34	1956	1990
Baker Lake*	**−0.098**	**−1.712**	**66**	**−0.411**	**−1.893**	**33**	1925	1989
Lake of the Woods	**0.341**	**2.659**	**43**	**0.552**	**2.778**	**29**	1956	1990
Island Lake*	−0.429	0.306	32	−0.429	0.306	32	1971	1988
Red Lake*	−0.188	−1.100	43	−0.200	−0.743	34	1956	1991
Big Trout Lake*	−0.188	−1.585	54	**−0.400**	**−1.895**	**33**	1947	1991
Attawapiskat Lake	−0.071	−0.338	53	−0.235	−1.039	34	1948	1988
Lake Timiskaming	0.800	0.948	20	0.800	−0.948	20	1990	1995
Lake Nipissing	0.400	−0.752	48	0.485	−0.666	34	1956	1988
Lake Muskoka	0.250	−0.783	20	0.250	−0.783	20	1900	1994
Lake Simco*	0.195	−1.017	68	**0.636**	**2.748**	**28**	1901	1995
Lac Nitchequon	**0.167**	**1.807**	**54**	0.455	−0.568	33	1947	1984
Lac Saint-Louis	0.035	−0.041	57	0.214	0.121	21	1920	1980
Lac Saint-Jean*	0.107	0.252	38	−0.150	−0.325	32	1965	1996
Far North								
Amadjuak Lake	0.500	0.87924	20					
Angajurjualuk Lake	0.529	0.37084	20					
Stanwell–Fletcher Lake	0.300	0.91423	19					
Washburn Lake	0.667	**2.04757**	**18**					
Sitidgi Lake	0.818	**2.2917**	**20**					
Lake Hazen	**1.750**	**3.35059**	**20**					

An * indicates lakes that that were calibrated using overlapping data.
Bold identifies lakes that were significant at the 90% confidence interval.

0.12 days/year for lakes showing a trend towards later FUE. For the period 1970–2004, 23 showed a trend towards later FUE, 11 were significant, and the average rate of change increased to 0.16 days/year. Spatially, FUE was much more heterogeneous owing to the dependence on factors discussed previously and differences in temperature changes during the freeze-up period. Temperature changes have been most pronounced in winter and spring, periods that have the greatest impact on BUE, whereas summer and fall temperatures that affect FUE have changed much less (Serreze et al., 2000). Thus, temperature may have exhibited less forcing on FUE compared to BUE and may be a partial explanation for the greater spatial variability. The results are in agreement with those reported by Duguay et al. (2006) where a regional trend of later FUE in southern Ontario and Quebec was found that also corresponds to increased summer temperatures in the region reported in Serreze et al. (2000). Increased summer temperatures increase the thermal capacity of the lake and the heat loss required for freezing to occur (Jeffreis et al., 2005). The results also support the increase in variability observed by Magnuson et al. (2000), where of the 26 lakes for which the comparison could be made, 17 showed an increase in variability comparing the complete record to the record for 1970–2004.

For the lakes in the far north, all showed a trend towards later FUE and three were statistically significant. The average change in FUE was, as in the case of BUE, considerably higher than that for the rest of Canada (0.76 days/year) adding further support to the potential warming effects in this region.

4. Summary and conclusions

Remote sensing time series are an important component of the Global Climate Observing System and are recognized as having significant theoretical and applied utility for studying climate variability and change. Satellite data can complement in-situ measurements providing long-term observations, continuity and consistency over large spatial regions at potentially lower cost than other methods. However, assembling satellite data records for climate studies is resource intensive requiring processing of large data volumes to generate geometrically and radiometricaly consistent time series.

In this study an automated methodology to estimate phenology events was developed that made use of a recently established comprehensive satellite data archive at the Canada Center for Remote Sensing. Comparison of satellite and in-situ observations of lake ice phenology events showed that ice break-up could be extracted from AVHRR time series with high accuracy. The other events BUS, FUS, FUE are also related to in-situ observations, but not as strongly as BUE due to the nature of the event or limitations of the satellite data record caused by the low sun elevation during the start and end of freeze-up and limitations in the in-situ record/observation methods.

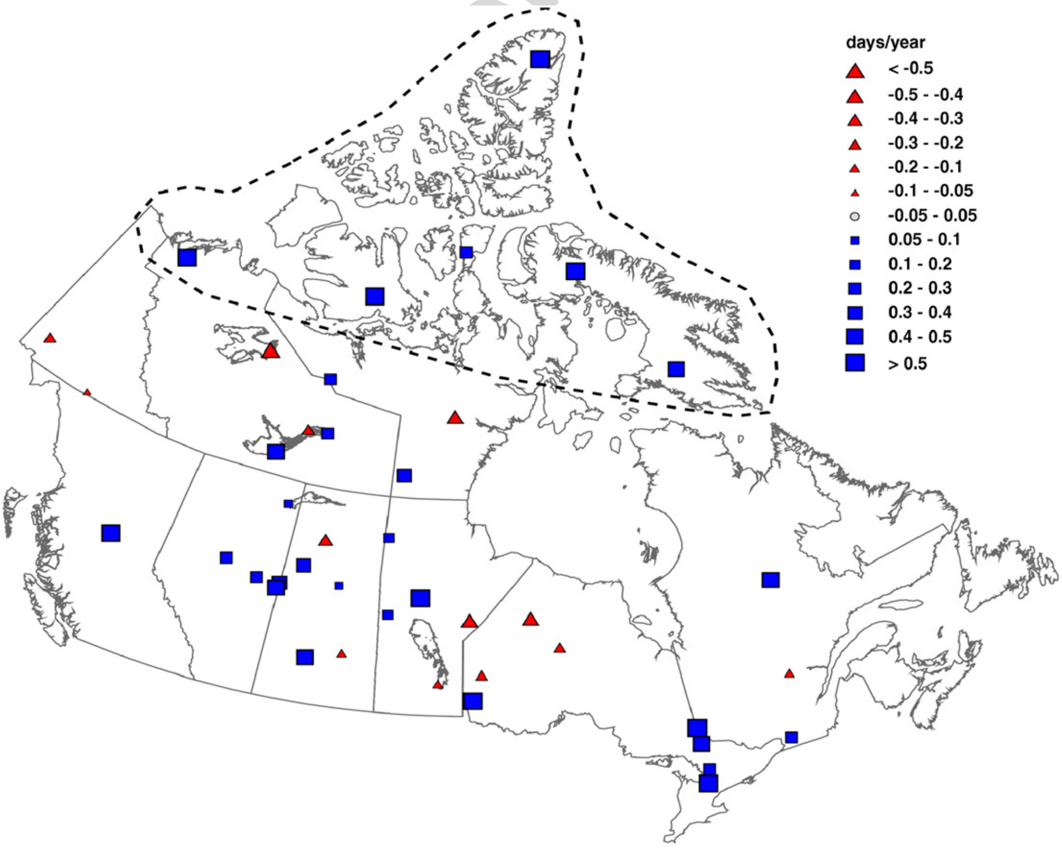

Fig. 11. Spatial pattern of freeze-up trends for the period 1970–2005. Dashed line identifies lakes in the far north for which only a 20 year remote sensing record was available.

Trend analysis performed using combined remote sensing and in-situ data shows that ice break-up is occurring earlier and freeze-up latter for most lakes in Canada with regional differences between eastern, western and the far northern regions. The later appears to be experiencing the most change, but further monitoring is required to develop a record of sufficient length to facilitate a conclusive evaluation.

Acknowledgements

We would like to thank Richard Fernandes for his input to the automated processing methodology and Vladimir Korolevich for assistance with the statistical trend analysis. We would also like to thank Andrew Davidson, Gunar Fedosejevs, Sylvain Leblanc, and Ian Olthof for their reviews of the manuscript. This work was completed under the NRCan/ESS Program, Enhancing Resilience in a Changing Climate and partially supported by Canadian Space Agency.

References

Anderson, W. L., Robertson, D. M., & Magnuson, J. J. (1996). Evidence of climatic change and projected future change. *Limnology and Oceanography*, *41*, 815−821.

Benson, B., & Magnuson, J. (2000). *Global lake and river ice phenology database.* Boulder, CO: National Snow and Ice Data Center/World Data Center for Glaciology Digital media.

Brown, R. D., & O'Neill, D. (2002). National plan for cryospheric monitoring — a Canadian contribution to the Global Climate Observing System. *Meteorological service of Canada, climate research branch, climate processes and earth observations division, Downsview, Ontario*.

Davidson, A., Wang, S. & Latifovic R. (2006). Extracting features of lake ice phenology over Canada from daily AVHRR observations, paper presented at Canadian Meteorological and Oceanographic Society Annual Meeting, Toronto, Canada, 29 May— 1 June 2006.

Duguay, C. R., & Lafleur, P. M. (1997). Determining depth and ice thickness of shallow sub-Artic lakes using space-borne optical and SAR data. *International Journal of Remote Sensing*, *24*, 475−489.

Duguay, C. R., & Lafleur, P. M. (2003). Determining depth and ice thickness of shallow sub-Artic lakes using space-borne optical and SAR data. *International Journal of Remote Sensing*, *24*, 475−489.

Duguay, C. R., Prowse, T. D., Bonsal, B. R., Brown, R. D., Lacroix, M. P., & Menard, P. (2006). Recent trends in Canadian lake ice cover. *Hydrological Processes*, *20*, 781−801.

Duguay, C. R., Pultz, T. J., Lafleur, P. M., & Drai, D. (2002). RADARSAT backscatter characteristics of ice growing on shallow sub-Artic lakes, Churchill, Manitoba, Canada. *Hydrological Processes*, *16*, 1631−1644.

Hall, D. K. (1998). Remote sensing of snow and ice. In F. M. Henderson & A.J. Lewis (Eds.), *Principles and applications of imaging radarManual of Remote Sensing*, *Vol. 2*. (pp. 677−703) Inc., New York: John Wiley & Sons.

Hall, D. K., Fagre, D. G., Klasner, F., Linebaugh, G., & Liston, G. E. (1994). Analysis of ERS 1 synthetic aperture radar data of frozen lakes in northern Montana and implications for climate studies. *Journal of Geophysical Research*, *99*, 22473−22482.

Hansen, J., Ruedy, R., Glascoe, J., & Sato, M. (1999). GISS analysis of surface temperature change. *Journal of Geophysical Research*, *104*, 30,997−31,022.

Jeffreis, M. O., Morris, K., & Kozlenko, N. (2005). Ice characteristics and processes, and remote sensing of frozen rivers and lakes. In C. R. Duguay & A. Pietroniro (Eds.), *Remote sensing in northern hydrology measuring environmental change* (pp. 63−90). Washington, DC: American Geophysical Union.

Jeffreis, M. O., Morris, K., Weeks, W. F., & Wakabayashi, H. (1994). Structural and stratigraphic feature and ERS 1 synthetic aperture radar backscatter characteristics of ice growing on shallow lakes in NW Alaska, winter 1991–1992. *Journal of Geophysical Research*, *99*, 22459−22471.

Kendall, M. G. (1975). *Rank Correlation Methods.* London: Charles Griffin.

Khlopenkov, K., & Trishchenko A.P. (accepted for publication) SPARC: New cloud, clear-sky, snow/ice and cloud shadow detection scheme for historical AVHHR 1-km observations over Canada. Journal of Atmospheric and Oceanic technology.

Klein, A. G., Hall, D. K., & Nolin, A. W. (2000). Development of a prototype snow albedo algorithm for the NASA MODIS instrument. *Proceedings of the 57th Eastern Snow Conference, 18–19 May 2000* (pp. 143−157). NY: Syracuse.

Latifovic, R., Cihlar, J., & Chen, J. (2003). Comparison of BRDF models for the normalization of satellite optical data to a standard sun-target-sensor geometry. *IEEE Transactions on Geoscience and Remote Sensing*, *41*, 1889−1898.

Latifovic, R., Trishchenko, A., Chen, J., Park, W., Khlopenkov, K., Fernandes, R., et al. (2005). Generating historical AVHRR 1 km baseline satellite data records over Canada suitable for climate change studies. *Canadian Journal of Remote Sensing*, *31*, 324−348.

Lenormand, F., Duguay, C. R., & Gauthier, R. (2002). Development of a historical database for the study of climate change in Canada. *Hydrological Processes*, *16*, 3707−3722.

Livingstone, D. M. (1997). Break-up of alpine lakes as proxy data for local and regional mean surface air temperatures. *Climatic Change*, *37*, 407−439.

Nolan, M., Liston, G., Prokein, P., Brigham-Grette, J., Sharpton, V. L., & Huntzinger, R. (2002). Analysis of lake ice dynamics and morphology on Lake El'gygytgyn, NE Siberia, using synthetic aperture radar (SAR) and Landsat. *Journal of Geophysical Research*, *108*, 3-1−3-12.

Magnuson, J. J., Benson, B. J., & Kratz, T. K. (1990). Temporal coherence in the limnology of a suite of lakes in Wisconsin, U.S.A. *Freshwater Biology*, *23*, 145−159.

Magnuson, J. J., Robertson, D. M., Benson, B. J., Wayne, R. H., Livingstone, D. M., Arai, T., et al. (2000). Historical trends in lake and river ice cover in the northern hemisphere. *Science*, *289*, 1743−1746.

Magnuson, J. J., Webster, K. E., Assel, R. A., Bowser, C. J., Dillon, P. J., Eaton, J. G., et al. (1997). Potential effects of climate changes on aquatic systems: Laurentian Great Lakes and Precambrian Shield region. *Hydrological Processes*, *11*, 825−871.

Mann, H. B. (1945). Non-parametric tests against trend. *Econometrica*, *13*, 245−259.

Maslanik, J. A., & Barry, R. G. (1987). Lake ice formation and break-up as an indicator of climate change: Potential for monitoring using remote sensing. *The influence of climate change and climate variability on the hydrologic regime and water resourcesInternational Association for the Hydrological Sciences*, *Vol. 168*. (pp. 153−168).

Mathworks (2006). http://www.mathworks.com, visited 10/04/2006.

McFadden, J. D. (1995). *The Interrelationship of Lake Ice and Climate in Central Canada. Technical report number*, *Vol. 20*. Office of Naval Research.

Morris, K., Jeffries, M. O., & Weeks, W. F. (1995). Ice processes and growth history on artic and sub-artic lakes using ERS-1 SAR data. *Polar Record*, *31*, 115−128.

Pavelsky, T. M., & Smith, L. C. (2004). Spatial and temporal patterns in Artic river ice breakup observed with MODIS and AVHRR time series. *Remote Sensing of Environment*, *93*, 328−338.

Robertson, D.M. (1989). The use of lake water temperature and ice cover as climatic indicators. PhD Dissertation, University of Wisconsin.

Rouse, W. R., Oswald, C. J., Binyamin, J., Spence, C., Schertzer, W. M., Blanken, P. D., et al. (2005). The role of northern lakes in a regional energy balance. *Journal of Hydrometeorology*, *6*, 219−305.

Sen, P. K. (1968). Estimates of the regression coefficient based on Kendall's tau. *Journal of the American Statistical Association*, *63*, 1379−1389.

Serreze, M. C., Walsh, J. E., Chapin, F. S., III, Osterkamp, T., Dyurgerov, M., & Romanovsky, V. (2000). Observational evidence of recent changes in the northern high-latitude environment. *Climatic Change*, *46*, 159−207.

Scambos, T., Haran, T., Fowler, C., Maslanik, J., Key, J., & Emery, W. (2000). *Updated 2002 AVHRR Polar Pathfinder twice-daily 1.25 km EASE-Grid composites.*Boulder, CO: National Snow and Ice Data Center Digital media.

Schindler, D. W., Beaty, K. G., Fee, E. J., Cruikshank, D. R., DeBruyn, E. R., Findlay, D. L., et al. (1990). Effects of climate warming on lakes of the central boreal forest. *Science*, *250*, 967−970.

Scott, J.T. (1964). A comparison of the heat balance of lakes in winter. PhD Dissertation, University of Wisconsin.

Walker, A. E., & Davey, M. R. (1993). Observation of Great Salve Lake ice freeze-up and break-up processes using passive microwave satellite data. *Proceedings of the 16th Canadian Remote Sensing Symposium, 7–10 June, Sherbrooke* (pp. 233−238). Canada: Quebec.

Wynne, R. H., & Lillesand, T. M. (1993). Satellite observation of lake ice as a climate indicator: Initial results from statewide monitoring in Wisconsin. *Photogrammetric Engineering and Remote Sensing*, *59*, 1023−1031.

Wynne, R. H., Lillesand, T. M., Clayton, M. K., & Magnuson, J. J. (1998). Satellite monitoring of lake ice breakup on the Laurentian Shield (1990–1994). *Photogrammetric Engineering and Remote Sensing*, *64*, 607−617.

Wynne, R. H., Magnuson, J. J., Clayton, M. K., Lillesand, T. M., & Rodman, D. C. (1996). Determinants of temporal coherence in the satellite-derived 1987–1994 ice breakup dates of lakes on the Laurentian Shield. *Limnology and Oceanography*, *41*, 832−838.

Yue, S., Pilon, P., & Cavadias, G. (2002). Power of the Mann–Kendal and Spearman's rho tests for detecting monotonic trends in hydrological series. *Journal of Hydrology*, *259*, 254−271.

Yue, S., Pilon, P., & Phinney, B. (2003). Canadian streamflow trend detection: Impacts of serial and cross-correlation. *Hydrological Sciences*, *48*, 51−63.